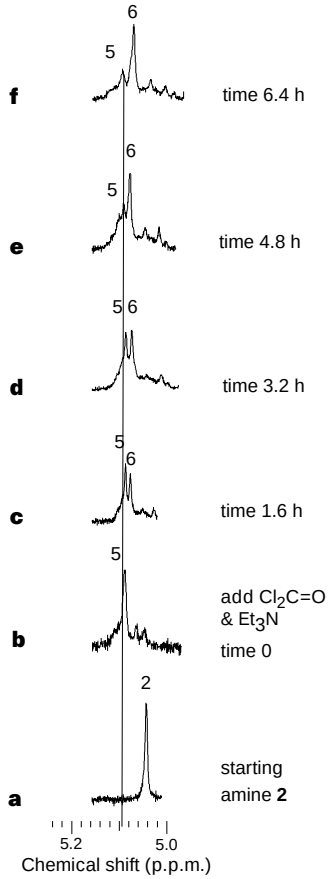

Figure 5 Spectroscopic evidence that carbonyl dichloride fuels the unidirectional rotation of **2**. Partial ^{1}H NMR spectra (monitoring the bridgehead proton relative to $(CH_3)_4Si$=0 p.p.m.) indicate the sequence of events as a function of time. Numbers next to peaks in the spectra refer to structures in Fig. 3. **a**, **2** in $CDCl_3$; **b**, t_0; addition of Cl_2C=O and Et_3N. **2** is rapidly converted to intramolecular urethane **5** via isocyanate **3**; the isocyanates **3** and **4** convert to **5** too rapidly to be seen in the spectra. **c**, After 1.6 h at ambient temperature (~22 °C), ~30% of **5** has rotated ''over the hump'' (Fig. 2d to Fig. 2f) to **6**. **d**, **e**, **f**, Over further time, rotation of **5** to **6** continues, with unidirectional conversion of **5** to **6** being >80% complete in ~6 h. Urethane **6** was isolated and shown to be identical to material prepared directly from amine rotamer **7** by reaction with Cl_2C=O/Et_3N. Control experiments established that **6** does not convert to **5**; that is, that the conversion of **5** → **6** is unidirectional. The assignment of structures to **3**–**6** is corroborated by infrared spectroscopic monitoring of the relevant reactions of **2**, **7** and **9** with Cl_2C=O/NEt_3 (and also **10** in the case of **9**), performed using ReactIR technology (ASI Applied Systems, Millersville, Maryland, USA); this equipment makes it possible to record *in situ*, and in real time, the infrared spectra of reaction mixtures and to thereby assay functional group changes as they occur.

treatment of **7** with Cl_2C = O/Et_3N leads rapidly to **6**, but **6** does not detectably convert to **5**). Finally, **6** is cleaved to give **7**, thereby completing the chemically driven rotation of **2** to **7**. Control experiments demonstrate that in the absence of Cl_2C=O/Et_3N, pure **2** slowly converts (over several days) to an approximately 1:0.8:1 equilibrium mixture of **2**, **7** and **8** (the third low-energy rotamer: see Fig. 4). In Fig. 5 we show the experimental data which establish that the events in Fig. 3 proceed as indicated. □

Received 11 March; accepted 16 July 1999.

1. Rayment, I. *et al.* Structure of the actin-myosin complex and its implications for muscle contraction. *Science* **261,** 58–65 (1993).
2. Abrahams, J. P., Leslie, A. G. W., Lutter, R. & Walker, J. E. Structure at 2.8 Å resolution of F_1-ATPase from bovine heart mitochondria. *Nature* **370,** 621–628 (1994).
3. Dominguez, R., Freyzon, Y., Trybus, K. M. & Cohen, C. Crystal structure of a vertebrate smooth muscle myosin motor domain and its complex with the essential light chain: visualization of the pre-power stroke state. *Cell* **94,** 559–571 (1998).
4. Block, S. M. Real engines of creation. *Nature* **386,** 217–219 (1997).
5. Noji, H., Yasuda, R., Yoshida, M. & Kinoshita, K. Jr Direct observation of the rotation of F_1-ATPase. *Nature* **386,** 299–302 (1997).
6. Boyer, P. D. The ATP synthase—a splendid molecular machine. *Annu. Rev. Biochem.* **66,** 717–749 (1997).
7. Shingyoji, C., Higuchi, H., Yoshimura, M., Katayama, E. & Yanagida, T. Dynein arms are oscillating force generators. *Nature* **393,** 711–714 (1998).
8. Berg, H. C. Keeping up with F_1-ATPase. *Nature* **394,** 324–325 (1998).
9. Vale, R. D. & Oosawa, F. Protein motors and Maxwell's demons: does mechanochemical transduction involve a thermal ratchet? *Adv. Biophys.* **26,** 97–134 (1990).
10. Stryer, L. in *Biochemistry* Ch. 15, 4th edn (W. H. Freeman, New York, 1995).
11. Howard, J. Molecular motors: structural adaptations to cellular functions. *Nature* **389,** 561–567 (1997).
12. Huxley, A. How molecular motors work in muscle. *Nature* **391,** 239–240 (1998).
13. Faucheux, L. P., Bourdieu, L. S., Kaplan, P. D. & Libchaber, A. J. Optical thermal ratchet. *Phys. Rev. Lett.* **74,** 1504–1507 (1995).
14. Travis, J. Making light work of Brownian motion. *Science* **267,** 1593–1594 (1995).
15. Astumian, R. D. Thermodynamics and kinetics of Brownian motion. *Science* **276,** 917–922 (1997).
16. Rousselet, J., Salome, L., Ajdari,k A. & Prost, J. Directed motion of brownian particles induced by a periodic asymmetric potential. *Nature* **370,** 446–448 (1994).
17. Mislow, K. Molecular machinery in organic chemistry. *Chemtracts—Org. Chem.* **2,** 151–174 (1989).
18. Bedard, T. C. & Moore, J. S. Design and synthesis of molecular turnstiles. *J. Am. Chem. Soc.* **117,** 10662–10671 (1995).
19. Balzani, V., Gomez-Lopez, M. & Stoddard, J. F. Molecular machines. *Acc. Chem. Res.* **31,** 405–414 (1998).
20. Sauvage, J.-P. Transition metal-containing rotaxanes and catenanes in motion: toward molecular machines and motors. *Acc. Chem. Res.* **31,** 611–619 (1998).
21. Bissell, R. A., Cordova, E., Kaifer, A. & Stoddart, J. F. A chemically and electrochemically switchable molecular shuttle. *Nature* **369,** 133–137 (1994).
22. Benniston, A. C. & Harriman, A. A light-induced molecular shuttle based on a [2]rotaxane-derived triad. *Angew. Chem. Int. Edn. Engl.* **32,** 1459–1461 (1993).
23. Mao, C., Sun, W., Shen, Z. & Seeman, N. C. A nanomechanical device based on the B-Z transition of DNA. *Nature* **397,** 144–146 (1999).
24. Kelly, T. R., Tellitu, I. & Sestelo, J. P. In search of molecular ratchets. *Angew. Chem. Int. Edn. Engl.* **36,** 1866–1868 (1997).
25. Kelly, T. R., Sestelo, J. P. & Tellitu, I. New molecular devices: in search of a molecular ratchet. *J. Org. Chem.* **63,** 3655–3665 (1998).
26. Davis, A. P. Tilting at windmills? The second law survives. *Angew. Chem. Int. Edn. Engl.* **37,** 909–910 (1998).
27. Musser, G. Taming Maxwell's demon. *Sci. Am.* **280,** 24 (1999).
28. Kelly, T. R. *et al.* A molecular brake. *J. Am. Chem. Soc.* **116,** 3657–3658 (1994).

Acknowledgements

We thank S. Jasmin and Y. Zhao for contributions to the preparation of necessary quantities of **2**, and J. Sieglen and B. Wang for technical assistance. This work was supported by the NIH.

Correspondence and requests for materials should be addressed to T.R.K. (e-mail: ross.kelly@bc.edu).

Light-driven monodirectional molecular rotor

Nagatoshi Koumura*†, Robert W. J. Zijlstra*, Richard A. van Delden*, Nobuyuki Harada† & Ben L. Feringa*

** Department of Organic and Molecular Inorganic Chemistry, Stratingh Institute, University of Groningen, Nijenborgh 4, 9747 AG Groningen, The Netherlands*
† Institute for Chemical Reaction Science, Tohoku University, 2-1-1 Katahira, Aoba, Sendai 980-8577, Japan

Attempts to fabricate mechanical devices on the molecular level[1,2] have yielded analogues of rotors[3], gears[4], switches[5], shuttles[6,7], turnstiles[8] and ratchets[9]. Molecular motors, however, have not yet been made, even though they are common in biological systems[10]. Rotary motion as such has been induced in interlocked systems[11–13] and directly visualized for single molecules[14], but the controlled conversion of energy into unidirectional rotary motion has remained difficult to achieve. Here we report repetitive, monodirectional rotation around a central carbon–carbon double bond in a chiral, helical alkene, with each 360° rotation involving four discrete isomerization steps activated by ultraviolet light or a change in the temperature of the system. We find that

axial chirality and the presence of two chiral centres are essential for the observed monodirectional behaviour of the molecular motor. Two light-induced *cis-trans* isomerizations are each associated with a 180° rotation around the carbon–carbon double bond and are each followed by thermally controlled helicity inversions, which effectively block reverse rotation and thus ensure that the four individual steps add up to one full rotation in one direction only. As the energy barriers of the helicity inversion steps can be adjusted by structural modifications, chiral alkenes based on our system may find use as basic components for 'molecular machinery' driven by light.

The structure of the molecular rotor (3*R*,3′*R*)-(*P*,*P*)-*trans*-1,1′,2,2′,3,3′,4,4′-octahydro-3,3′-dimethyl-4,4′-biphenanthrylidene (**1** in Fig. 1) features two identical halves connected by a central carbon-carbon double bond. (Here *P* denotes the right-handed helicity in each half of the structure; *M*, used later, stands for left-handed helicity.) The design of the molecular rotor presented here is based on the exploitation of two fundamental principles. First, the light-induced *trans* to *cis* isomerization around a carbon–carbon double bond is an extremely fast and reversible process; in nature, it forms the basis for the information-retrieval step in the process of vision. Second, the concerted action of two chiral elements in a single chemical or physical event can lead to a unique handedness via the process of chiral discrimination, one of the essential features in living organisms. Steric interference in the molecule imposes a helical shape to the structure. *Trans*-**1** and *cis*-**2** are isomeric structures following a 180° rotation around the central bond, a process which is accomplished by irradiation with ultraviolet light at room temperature.

The configuration at the stereogenic centre, bearing the methyl-substituent, is (*R*) for both halves; Me_{ax} and Me_{eq} (Fig. 1) are axial and equatorial oriented methyl-substituents, respectively. The synthesis of *trans*-(3*R*,3′*R*)-(*P*,*P*)-**1** and the unequivocal determination of the absolute stereochemistry and molecular structures of *trans*-**1** and *cis*-**2** have been reported[15]. We studied the photochemical switching behaviour of **1**, and Fig. 1 shows the dynamic processes and the different stereoisomeric structures that were observed. The absorption spectra of the stereoisomers of **1** and **2** are given in Fig. 2.

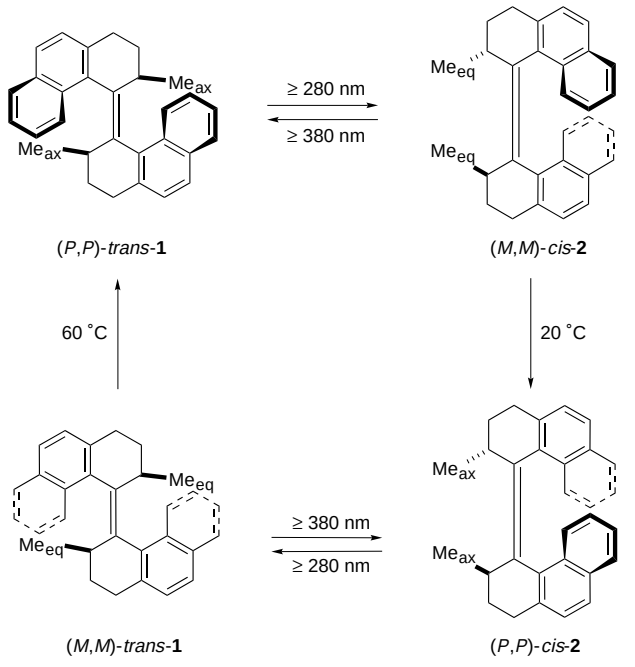

Figure 1 Photochemical and thermal isomerization processes of (*P*,*P*)-*trans*-**1**. UV irradiation with high pressure Hg-lamp, Pyrex filter, $\lambda \geq 280$ nm or Xe-lamp, Toshiba L-3g glass filter, $\lambda \geq 380$ nm. First order kinetics were observed for the thermal processes and temperature dependent ^{1}H NMR and CD studies in the range 50.0–81.1 °C gave Ea = 26.4 kcal mol^{-1} for the (*M*,*M*)-*trans*-**1** to (*P*,*P*)-*trans*-**1** interconversion. It should be noted that no racemization takes place during any of the photochemical or thermal steps as was proven by chiral HPLC analysis of the isomers obtained after the individual steps.

Irradiation (wavelength $\lambda \geq 280$ nm) of (*P*,*P*)-*trans*-**1** in *n*-hexane at −55 °C resulted in the formation of (*M*,*M*)-*cis*-**2**. A *cis*-**2** to *trans*-**1** ratio of 95:5 is observed at photoequilibrium. The isomerization is fully reversible, and the photoequilibrium shifts to (*P*,*P*)-*trans*-**1** as the main isomer on irradiation with $\lambda \geq 380$ nm. The *trans*–*cis* photoisomerization is evident from ^{1}H NMR analysis, and the simultaneous reversal of *P* to *M* helicity is detected by circular dichroism (CD) (Fig. 3, traces A and B).

When the temperature of the solution of (*M*,*M*)-*cis*-**2** is raised to 20 °C, a fast and selective conversion to (*P*,*P*)-*cis*-**2** is observed and the concomitant change in CD absorption (Fig. 3, traces B and C) shows the helix reversal associated with this thermal interconversion. Irradiation of (*P*,*P*)-*trans*-**1** under ambient conditions leads to complete conversion to (*P*,*P*)-*cis*-**2**, as the unstable (*M*,*M*)-*cis*-**2** is removed from the photoequilibrium in a fast thermal isomerization. Although (*P*,*P*)-*cis*-**2** was prepared by photochemical isomerization of (*P*,*P*)-*trans*-**1** (ref. 16) we have now established that there is no direct pathway between these isomers. It should be emphasized that the (*M*,*M*)-*cis*-**2** to (*P*,*P*)-*cis*-**2** isomerization is irreversible under the thermal or photochemical conditions that were employed. Subsequent irradiation of (*P*,*P*)-*cis*-**2** at $\lambda \geq 280$ nm results in the formation of (*M*,*M*)-*trans*-**1**, reaching a photoequilibrium with a ratio of (*M*,*M*)-*trans*-**1** to (*P*,*P*)-*cis*-**2** of 90:10. The change in CD absorption that accompanies this photochemical *cis*–*trans* isomerization (Fig. 3, traces C and D) is again associated with a *P*,*P* to *M*,*M* helicity reversal. When the temperature of a solution of (*M*,*M*)-*trans*-**1** was increased to 60 °C, (*P*,*P*)-*trans*-**1** was formed exclusively and the CD absorptions again change sign, reverting to the original values found in the spectrum of (*P*,*P*)-*trans*-**1**. The four changes in the sign of the CD absorption occur only around 217 nm (Fig. 3). The reverse mode of this process (that is, direct photochemical or thermal isomerization of (*P*,*P*)-*trans*-**1** to (*M*,*M*)-*trans*-**1**) is not observed.

The main question is why the thermal *M*,*M* to *P*,*P* double helix reversal for both the *trans*-isomer **1** and the *cis*-isomer **2** are irreversible. Molecular modelling studies (MOPAC 93-AM1, Fujitsu, Tokyo, 1993) of (3*R*,3′*R*)-*trans*-**1** show two stable forms, (*P*,*P*)-*trans*-**1** and (*M*,*M*)-*trans*-**1**, with an energy difference (ΔE) of 8.6 kcal mol^{-1} in favour of the (*P*,*P*)-isomer in accordance with the experimental observations. In the more stable (*P*,*P*)-isomer, the two methyl substituents are in axial positions (to prevent steric hindrance) whereas in the less stable (*M*,*M*)-isomer the methyl groups adopt equatorial orientations. For the *cis*-isomer **2** the two methyl groups are again in an axial orientation in the most stable (*P*,*P*)-*cis*-**2** form,

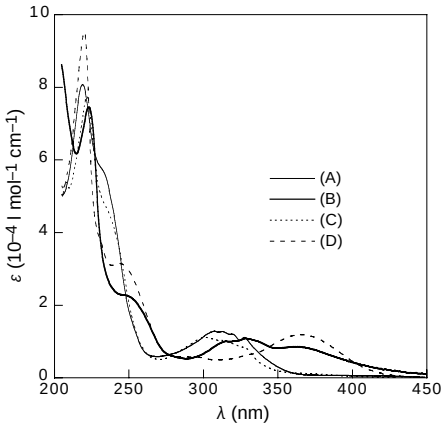

Figure 2 Ultraviolet–visible spectra (hexane solvent). Trace A, (*P*,*P*)-*trans*-**1**; trace B, (*M*,*M*)-*cis*-**2**; trace C, (*P*,*P*)-*cis*-**2**; trace D, (*M*,*M*)-*trans*-**1**.

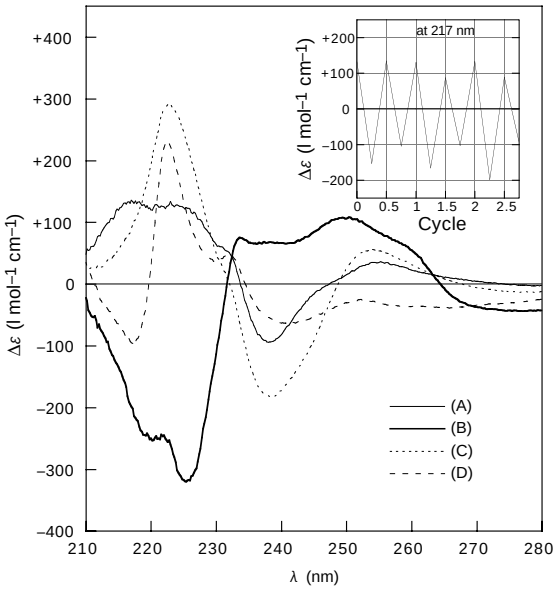

Figure 3 Circular dichroism (CD) spectra system in each of four stages of switching (see text). Trace A, (*P*,*P*)-*trans*-**1**; trace B (*M*,*M*)-*cis*-**2**; trace C, (*P*,*P*)-*cis*-**2**; trace D, (*M*,*M*)-*trans*-**1**. Inset, change in CD signal during full rotation cycle of (*P*,*P*)-*trans*-**1** monitored at 217 nm.

whereas in the less stable (*M*,*M*)-*cis*-**2** form ($\Delta E = 11.0\,\mathrm{kcal\,mol^{-1}}$) the two methyl groups take equatorial positions.

The above results indicate that irradiation of (*P*,*P*)-*trans*-**1** at $\lambda \geqslant 280$ nm at 60 °C will result in the formation of all three other states of the four-step isomerization cycle (shown in Fig. 1) consecutively, because under these conditions both photoisomerization steps as well as the two thermal isomerization steps will take place. The inset of Fig. 3 shows the change in CD signal at 217 nm, as monitored during three full cycles. When one considers the structural changes observed during the full cycle shown in Fig. 1 it is evident that, relative to the bottom half of the molecule (considered the static part), the top half of the molecule (considered the rotor) undergoes a full 360° rotation exclusively in a clockwise sense (as seen from the side of the static part). To the best of our knowledge, this is the first observation of a monodirectional photochemically driven rotation of a propeller-type unit, and it shows that controllable rotatory motion can be produced by the influx of external energy[17].

The stereochemical changes during the entire rotation cycle that dictate the clockwise monodirectional behaviour for (*P*,*P*)-*trans*-**1** can be rationalized as follows. Photochemical *trans*–*cis* isomerization inverts the *P*,*P* helicity to *M*,*M* helicity. Simultaneously, the axial methyl substituents in (*P*,*P*)-*trans*-**1** adopt the less favourable equatorial orientation in (*M*,*M*)-*cis*-**2**. The photochemically induced—energetically uphill—process is followed by a thermal downhill process in which inversion of *M*,*M* to *P*,*P* helicity occurs, and the methyl substituents adopt the more favourable axial orientation. Next, a second photochemical step converts *cis*-**2** to *trans*-**1** with simultaneous *P*,*P* to *M*,*M* helix inversion; but in this step again, as a consequence of the rotation around the alkene double bond, the methyl groups adopt the less favourable equatorial orientation. Finally, (*M*,*M*)-*trans*-**1** relaxes to the starting isomer (*P*,*P*)-*trans*-**1** with simultaneous *M*,*M* to *P*,*P* helix inversion and a change of the less favourable equatorial to the more favourable axial orientation of the methyl groups.

The absorption of light energy and the unique combination of axial chirality and two chiral centres in this molecular rotor are essential for the observed monodirectional behaviour. Two light-driven steps induce rotations around the central alkene double bond and generate the less stable (*M*,*M*)-*cis*-**2** and (*M*,*M*)-*trans*-**1** isomers. Subsequently two energetically downhill processes generate the more stable (*P*,*P*)-*cis*-**2** and (*P*,*P*)-*trans*-**1** isomers. As the helicity inverts simultaneously in the last two steps, the reverse rotation pathway is effectively blocked. Starting with (3*R*,3′*R*)-(*P*,*P*)-**1**, clockwise rotation is therefore found; if the (3*S*,3′*S*)-(*M*,*M*)-**1** enantiomer of this molecular rotor were used, anti-clockwise rotation is expected.

The cycle shown in Fig. 1 may be regarded as four distinct states in an optical molecular switch, each of which can be populated depending upon temperature and wavelength of the light used; at the appropriate wavelength and temperature, a continuous monodirectional rotation is induced in the system. The origin of this rotation process lies in the molecular architecture of structure **1**, where the following stereochemical features are all important: thermally stable, but photochemically interconvertable *cis* and *trans* isomers; (*P*,*P*) or (*M*,*M*) helicity; the fixed (3*R*,3′*R*)-configuration at the stereogenic centres; conformational flexibility of the cycloalkene rings; and the axial or equatorial orientation that can be adopted by the methyl groups. □

Received 3 June; accepted 2 August 1999.

1. Feynman, R. P. in *Miniaturization* (ed. Gilbert, H. D.) (Reinhold, New York, 1961).
2. Drexler, K. E. *Nanosystems: Molecular Machinery, Manufacturing and Computation* (Wiley, New York, 1992).
3. Schoevaars, A. M. *et al.* Toward a switchable molecular rotor. *J. Org. Chem.* **62,** 4943–4948 (1997).
4. Clayden, J. & Pink, J. H. Concerted rotation in a tertiary aromatic amide: towards a simple molecular gear. *Angew. Chem. Int. Edn Engl.* **37,** 1937–1939 (1998).
5. Huck, N. P. M., Jager, W. F., de Lange, B. & Feringa, B. L. Dynamic control and amplification of molecular chirality by circularly polarized light. *Science* **273,** 1686–1688 (1996).
6. Bissell, S. A., Córdova, E., Kaifer, A. E. & Stoddart, J. F. A chemically and electrochemically switchable molecular shuttle. *Nature* **369,** 133–136 (1994).
7. Ashton, P. R. *et al.* Acid-base controllable molecular shuttles. *J. Am. Chem. Soc.* **120,** 11932–11942 (1998).
8. Bedard, T. C. & Moore, J. S. Design and synthesis of a "molecular turnstile". *J. Am. Chem. Soc.* **117,** 10662–10671 (1995).
9. Kelly, T. R., Tellitu, I. & Sestelo, J. P. In search of molecular ratchets. *Angew. Chem. Int. Edn Engl.* **36,** 1866–1868 (1997).
10. Noji, H., Yasuda, R., Yoshida, M. & Kinosita, K. Jr Directed observation of the rotation of F1-ATPase. *Nature* **386,** 299–302 (1997).
11. Balzani, V., Gómez-López, M. & Stoddard, J. F. Molecular machines. *Acc. Chem. Res.* **31**, 405–414 (1998).
12. Sauvage, J.-P. Transition metal-containing rotaxanes and catenanes in motion: toward molecular machines and motors. *Acc. Chem. Res.* **31,** 611–619 (1998).
13. Armaroli, N. *et al.* Rotaxanes incorporating two different coordinating units in their thread: synthesis and electrochemically and photochemically induced molecular motions. *J. Am. Chem. Soc.* **121,** 4397–4408 (1999).
14. Gimzewski, J. K. *et al.* Rotation of a single molecule within a supramolecular bearing. *Science* **281,** 531–533 (1998).
15. Harada, N., Koumura, N. & Feringa, B. L. Chemistry of unique chiral olefins. 3. Synthesis and absolute stereochemistry of trans- and cis-1,1′,2,2′,3,3′,4,4′-octahydro-3,3′-dimethyl-4,4′-biphenanthrylidenes. *J. Am. Chem. Soc.* **119,** 7256–7264 (1997).
16. Koumura, N. & Harada, N. Photochemistry and absolute stereochemistry of unique chiral olefins, trans- and cis-1,1′,2,2′,3,3′,4,4′-octahydro-3,3′-dimethyl-4,4′-biphenanthrylidenes. *Chem. Lett.*

1151–1152 (1998).
17. Davis, A. P. Tilting at windmills? The second law survives. *Angew. Chem. Int Edn Engl.* **37,** 909–910 (1998).

Correspondence and requests for materials should be addressed to B.L.F. (e-mail: B.L.Feringa@chem. rug.nl).

Acknowledgements

Financial support from the Netherlands Organisation for Scientific Research (NWO-STW) to B.L.F. is acknowledged.

Peacocks lek with relatives even in the absence of social and environmental cues

Marion Petrie*, Andrew Krupa† & Terry Burke†

** Evolution and Behaviour Research Group, Department of Psychology, University of Newcastle, Newcastle-upon-Tyne NE1 7RU, UK*
† Department of Animal and Plant Sciences, University of Sheffield, Sheffield S10 2TN, UK

Lek mating systems are characterized by males displaying in groups. The main benefit from group display is thought to be an increase in the number of females arriving per male. However, when mating success is highly skewed it is not clear why unsuccessful males participate in group display[1]. In theory, all males on leks could obtain indirect fitness benefits if displaying groups consisted of related individuals[2]. Here we present two independent sets of data that show that peacocks (*Pavo cristatus*) display close to their kin. DNA fingerprinting showed that males at Whipsnade Park were more closely related to males within the same lek than to males at other leks. Separately, we found that after an experimental release of a mixed group of related and unrelated males, brothers (paternal sibs or half-sibs) established permanent display sites very close together. This result is unexpected, as the released birds could not become familiar with their brothers during their development. The released young were hatched from eggs that had been removed from their parents shortly after laying and mixed with the eggs of non-relatives. These data indicate that birds can evolve a means of kin association that does not involve learning the characteristics of relatives or the use of environmental cues. If social learning is not necessary for kin association then kin effects may be of more widespread importance in avian social interactions, and in particular in the evolution of lek mating, than previously appreciated.

Males in lek mating systems aggregate to display to attract females. Group display has been shown to increase the number of females arriving per male in several lekking species[3,4], but, as a result of the skew in mating success, this does not always increase the number of matings for all of the participants under all circumstances[5]. Unsuccessful males appear only to be increasing the mating success of their more successful neighbours. However, they may gain inclusive fitness benefits from their display if they lek in association with relatives, and lekking may therefore be promoted by kin selection[2]. Here, we investigate whether peacock leks consist of relatives.

Peacocks were studied at Whipsnade Park, UK, where there is a population of around 200 free-ranging peafowl. Peacocks are a classic lekking species where groups of males aggregate at display sites and call together. Once females arrive on leks, males stop calling and display their upper tail coverts[6]; mating success is highly skewed, and most males on leks gain no matings. Peacocks establish permanent display sites in their fourth year. Males are present on their display sites for most of every day for the duration of the mating season, and return to the same site every year. Males can be as close as 2.5 m apart and, on one lek site in the park containing 10 individuals, males were on average 8.83 m (s.d. 6.50 m) apart[6]. We took blood samples from 21 displaying males distributed across four main lek sites (Fig. 1). We used multilocus fingerprinting to compare the genetic similarity (measured as the degree of band-sharing) within and between these lek sites. The degree of band-sharing within leks was significantly higher than that between leks (within leks mean $S = 0.816$, $n = 48$; between leks $S = 0.777$, $n = 162$; Mantel randomization test[7], 100,000 randomizations, $P = 0.01$; Fig. 2). Assuming that birds in different leks are unrelated and the detected minisatellites segregate independently, the increased band sharing within leks is close to that expected for half-siblings (0.810)[8].

How could peacocks come to display near to their close kin? Peacocks take no part in reproduction after mating and therefore young birds cannot learn the identity of their fathers. One possibility that could result in a tendency for related birds to display

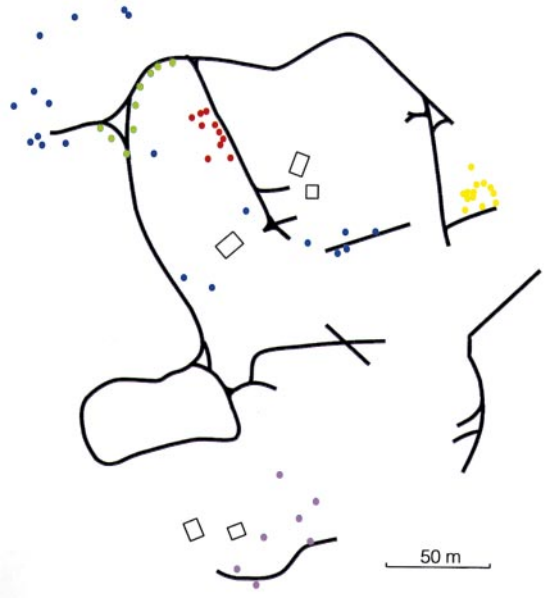

Figure 1 Distribution of 59 displaying male peacocks at Whipsnade Park in 1995 (excluding released males). Four leks (green, red, purple and yellow) were defined in the study area according to close visual contact between displaying males. Adjacent birds excluded from leks (blue) were obscured by topography, stands of trees or fencing.

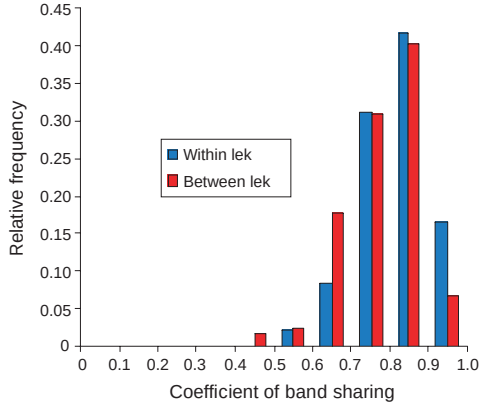

Figure 2 Comparison of band-sharing between individual multilocus minisatellite DNA profiles within (blue bars) and between (red bars) the display sites represented in Fig. 1. Peacocks displaying at the same lek ($n = 4$, 6, 4 and 7, respectively) were significantly more genetically similar to one another than they were to birds at other leks ($P = 0.01$).